ELSEVIER

Polymer 41 (2000) 6813–6824

polymer

Crystallization in modified blends of polyamide and polypropylene

J. Pigłowski[a,*], I. Gancarz[a], M. Wlaźlak[a], H.-W. Kammer[b]

[a]*Institute of Organic and Polymer Technology, Wrocław University of Technology, Wybrzeże Wyspiańskiego 27, 50-370 Wrocław, Poland*
[b]*School of Chemical Sciences, University Sains Malaysia, 11 800 Penang, Malaysia*

Received 16 September 1999; accepted 7 December 1999

Abstract

A modified polyamide 6 has been used as compatibilizer in blends of polyamide (PA) and isotactic polypropylene (PP). PA was modified in the molten state by trimellitic acid (TMA) and *n*-octyl glycidyl ether by reactive processing. NMR and FTIR results show that TMA and the ether reacted with PA. Isothermal crystallization kinetics of the polymers in neat and blend states has been investigated by differential scanning calorimetry. Crystallization behavior of the polymers in neat state differs from that in blends. However, tendencies are the same for the constituents. The rate of crystallization is highest in unmodified blends and lowest in neat polymers while intermediate in modified blends. An investigation of surface and interfacial tension revealed that both surface tension of modified PA and interfacial tension between modified PA and PP decrease as compared to unmodified PA. These results are consistent with optical micrographs that show finer dispersions of particles in modified than in unmodified systems.

Keywords: Polyamide; Polypropylene; Blends

1. Introduction

Blending of polyamide 6 (PA) and polypropylene (PP) is a challenging task since combination of properties of both polymers might be a promising route to generate materials with new characteristics. Both polymers are immiscible and form heterogeneous systems that display usually poor mechanical performance. Therefore, compatibilizing agents have to be used to reduce the interfacial tension and to improve the adhesion between the two constituents [1–4]. Lowering of interfacial tension simultaneously leads to finer dispersion of the minor component in the blend. The morphological stability of these blends depends critically on the level of compatibilizer. Blends of polyamide and polypropylene are most often compatibilized by maleic- and acrylic acid-grafted polypropylenes [5–7]. For compatibilizers containing maleic anhydride groups, the formation of succinimide group through amine–anhydride reaction has been demonstrated by IR [8].

Recently Eichhorn [9] described the fast process for controlled chemical degradation of polyamide with trimellitic anhydride in the melt. For the reaction of polyamide with anhydrides in the molten state two mechanisms are proposed in the literature [10,11]. The first one is the reaction of an anhydride with the amino end groups of PA and the second one is the amide–anhydride reaction that results in chain rupture. These reactions modify both the amino and carboxyl end group concentrations and the chain length.

Here, a PA, modified by trimellitic anhydride and an alkyl glycidyl ether, has been applied as compatibilizing agent. *n*-Octyl groups, additionally introduced into polyamide, affect the morphology of modified PA/PP blends. Even though PP and polyamide substituted with *n*-octyl groups are not miscible, one expects enhanced affinity between them that reduces interfacial tension and heterogeneity of the blends.

There are different variables that may affect the properties of PA/PP blends: the ratio of polyamide to polypropylene, the volume fraction of compatibilizer, the molecular weight of polyamide and polypropylene, composition and functionality of the compatibilizer and the crystalline structure of these systems [3,12,13]. This paper focuses on the crystallization behavior of PA/PP blends and on alterations of it caused by the compatibilizer. Knowledge of crystallization kinetics and crystalline structure of the blends is important for adjustment of their final properties. The morphology and mechanical properties of the modified PA/PP blends are also briefly mentioned.

2. Experimental

2.1. Materials

Isotactic polypropylene (Malen F 401) and polyamide 6

* Corresponding author. Fax: + 48-71-3203678.

0032-3861/00/$ - see front matter
PII: S0032-3861(00)00034-3

Table 1
Characteristics of the polymers

Polymer	Density (g/cm^3)	MFI (g/10 min)	Concentration of amino end groups (mval kg^{-1})	T_m° [a] (K)	ΔH_0 [b] ($J\,g^{-1}$)
PA	1.13	–	45–47	503	190 [15]
PP	0.91	2.4–3.2	–	481	137.9 [14]

[a] Apparent equilibrium melting temperature.
[b] Melting enthalpy of 100% crystalline material.

(Stilamid S-24) are commercial polymers that were supplied by Petrochemia Płock, S.A. (Poland) and Stilon S.A., Gorzów (Poland), respectively. The isotacticity of PP amounts to 95% determined by NMR. The characteristics of the polymers are given in Table 1.

A polyamide modified in the molten state by trimellitic anhydride and *n*-octyl glycidyl ether (PA–TMA10–C_8 glycidyl ether) was used as compatibilizer for the PA/PP blend. The number after the trimellitic anhydride abbreviation gives the relative amount of TMA (in wt.%) that was used for modification of PA during reactive processing.

2.2. Blend preparation

All polymer materials were dried at 90°C in vacuum overnight before blending. A Brabender-like apparatus was used to modify polyamide and to prepare PA/PP blends. A desired amount of TMA powder (1.1, 10, and 15 wt.%) and PA were mixed carefully and then filled in the mixing chamber at 240°C. Rotor speed and mixing time were fixed at 38 rpm and 5 min, respectively. Then the mixture was cooled to 220°C and 6 wt.% of C_8 glycidyl ether was added. Mixing was continued for 5 min (until no volatile mist was observed). The modified polyamide is coded as PA–TMA Y–C_8 glycidyl ether, where Y corresponds to wt.% of trimellitic anhydride that was used.

All reactive processing procedures were done under nitrogen. Moreover, 1 wt.% of antioxidant (Lovinox HD 98) was added to reduce thermal oxidation.

2.3. Thermal analysis

The glass transition (T_g), the observed melting temperatures (T_m) and the crystallinity index (X) of pure PA and PP as well their blends were obtained by using a Mettler Toledo TA 821[e] differential scanning calorimeter.

The following thermal histories were imposed: samples of pure PA and modified PA blends (about 15 mg) were heated from −70 up to 240°C at a rate of 10 K min^{-1} and the heat (dH/dt) evolved during the scanning process was recorded as a function of temperature. For neat PP, the measurement was done only up to 190°C. The inflection point of the glass transition was taken as T_g. The melting temperature T_m and the enthalpies of fusion (ΔH) were obtained from the maximum and area of the endothermic peaks, respectively.

For studies of crystallization kinetics in blends, a two-step procedure was applied. The samples were annealed at 240°C for 5 min. Afterwards, the samples were cooled at a rate of −70 K min^{-1} to the preset crystallization temperature of PA. After isothermal crystallization of PA, PP was isothermally crystallized in an analogous procedure. The crystallization heat was recorded in terms of time required until the crystallization was completed or until any heat liberated was too small to be detected. The partial areas, corresponding to a particular degree of crystalline transformation, were determined using the Mettler Toledo analysis software.

2.4. Spectral analysis

PA and modified samples were purified by dissolution in formic acid and precipitation into distilled water, then dried in vacuum at 90°C to constant weight.

Polymer films obtained in a press at 220°C and under 100 atm for 5 min, were used for FTIR–ATR analysis. Spectra were recorded on Perkin–Elmer System 2000 apparatus with Spectra Tech ATR device (german 45°). Thirty two scans with 4 cm^{-1} resolution were taken. The absorbance at 1543 cm^{-1} (amide II NH groups), 1637 cm^{-1} (amide I CO groups), 1716 cm^{-1} (C=O of cyclic aromatic imides) 2936 and 2868 cm^{-1} (CH_2 groups) were measured. The last two peaks were adopted as standard peaks.

For ^{1}H-NMR analysis, about 0.03 g of polymer dissolved in 0.6 ml of deuterated trifluoroacetic acid was used. A qualitative estimation of the degree of modification is based on the spectra recorded with an AMX 300 MHz Bruker apparatus.

2.5. Other measurements

A scanning electron microscope JEOL ISM 5800 LV was used to examine the morphology of the blends. The specimens were broken under liquid nitrogen and fractured surfaces were gold coated and observed under an electron microscope.

The surface tension of the investigated samples (at room temperature) was determined from advancing contact angles of two probe liquids: distilled water and methylene iodide.

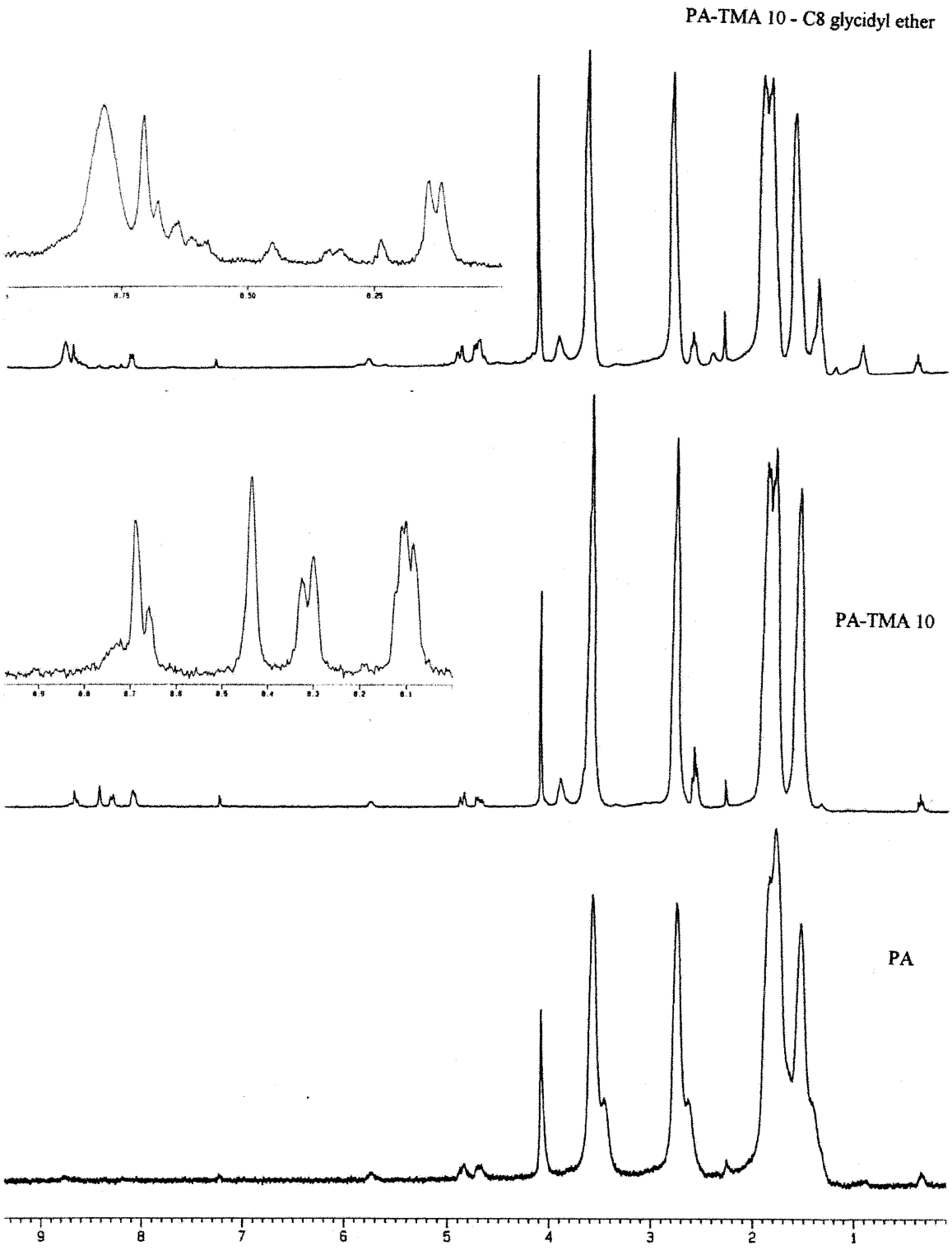

Fig. 1. ^{1}H-NMR spectra of PA, PA–TMA10 and PA–TMA10–C_8 glycidyl ether.

Measurements were carried out under an air atmosphere using an optical system consisting of a Panasonic GL 350 camera connected to a Technicome board that performed the drop shape analysis. For molten samples, measurements of interfacial tension were carried out in a heated cell at 235°C. The contact angle was measured that developed between a molten PA-hemisphere, having a radius of 2–4 mm, and a thin PP film coating a plane surface of cover glass. Nitrogen atmosphere was applied to prevent polymer oxidation.

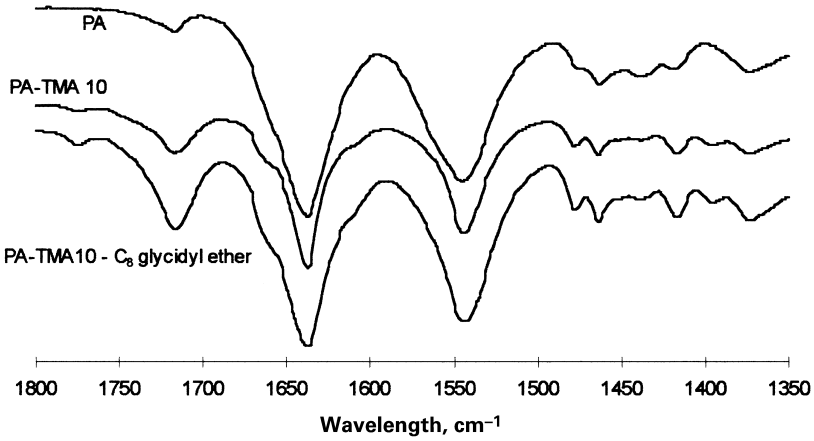

Fig. 2. FTIR spectra for PA, PA–TMA10 and PA–TMA10–C_8 glycidyl ether.

Measurement of tensile properties was carried out according to ISO 527-1 with a TIRA*test* 2705 at a crosshead speed of 10 mm min^{-1}.

3. Results and discussion

3.1. NMR and FTIR studies

^{1}H-NMR analysis was performed on samples purified to remove any anhydride not chemically bonded to the polyamide. The spectra of pure polyamide, polyamide modified with trimellitic anhydride and polyamide modified with TMA and then with C_8 glycidyl ether are shown in Fig. 1. One may recognize that in all modified samples aromatic groups are present. The amounts of attached anhydride and glycidyl ether calculated on the basis of NMR integration values correspond to the amounts added to PA. It means that within the limits of NMR accuracy, the total amount of TMA and glycidyl ether added to the molten polyamide reacts with it. We note that more than three signals occur in the aromatic region of the sample PA–TMA10. Three peaks are expected if exclusively imide or amide structures were present. More than three shifts probably means that the chain ends of the modified polyamide contain both of them or some side reaction takes place. The presence of C_8 glycidyl ether in the modified polyamide is manifested by signals at 0.9 ppm (CH_3 groups) and at 1.36 ppm (CH_2 groups). The spectra of two modified polymers (PA–TMA10 and PA–TMA10–C_8 glycidyl ether) differ significantly from each other. It suggests that glycidyl addition changed the course of the reaction. Possibly, glycidyl groups react with polyamide ends under opening of the oxirane ring. Evolving hydroxyl groups could then react with trimellitic anhydride giving monoester groups. This would explain the more complicated aromatic region of ^{1}H-NMR spectrum than in the former case. However, a more detailed analysis requires additional studies.

Table 2
Thermal characteristics of neat PA, PP, modified PA and of blends

Sample	T_g (K)	T_m (K)	X
PA	325	495	0.40
PP	255	442	0.64
PA/PP (70/30) blend			
PA	324	494	0.31
PP	254	438	0.67
PA–TMA1.1	336	499	0.38
PA–TMA10	320	485	0.37
PA–TMA15	317	474	0.40
PA–TMA10–C_8 glycidyl ether	315	485	0.38
PA/PP/PA–TMA10–C_8 glycidyl ether (1/1/1) blend			
PA	318	494	0.36
PP	255	441	0.73

FTIR spectra of all the modified samples display a new band of low intensity at 1774 cm^{-1} and the band at 1717 cm^{-1} (present in PA as a shoulder) is more pronounced (Fig. 2). These two bands are characteristic of symmetric and asymmetric stretching vibrations of C=O groups belonging to the cyclic aromatic imides [9]. The ratio of absorption bands at 1543 cm^{-1} (amide II NH groups) and at 1637 cm^{-1} (amide I CO groups) versus absorption of CH_2 groups for anhydride modified samples is greater than in the case of unmodified PA. This fact would support the hypothesis that the imide ring formation does not proceed fully. When C_8 glycidyl ether was added the above mentioned ratio is equal to that for polyamide. The shoulder at about 1675 cm^{-1}, appearing in the spectrum of modified samples, may originate from aromatic acid C=O groups whereas bands at 1477 and 1395 cm^{-1} are related to C=C and C=C–H groups, respectively.

3.2. Thermal behavior

Differential scanning calometric (DSC) studies revealed that thermal characteristics and degrees of crystallinity of neat PA and PP only slightly change when they are

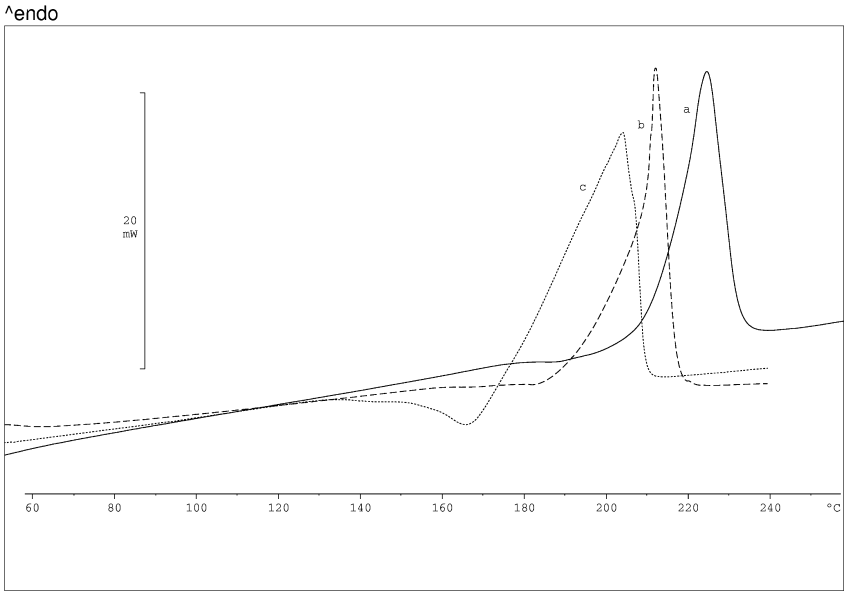

Fig. 3. DSC traces of reheating cycles for: (a) PA–TMA1.1; (b) PA–TMA10 and (c) PA–TMA15.

transformed into blends. The degree of crystallinity was calculated as the ratio of the melting enthalpies subdivided by the weight fraction w_i of the respective component in the blend, $X = \Delta H/(w_i \Delta H_0)$, where ΔH_0 is the melting enthalpy of 100% crystalline polymer. It turned out that the degree of crystallinity of PA in blends is slightly reduced while that of PP slightly increases (Table 2). However, a pronounced shift in crystallization temperature to higher temperatures was observed for PP (cf. Fig. 6). The modification of PA, with different amounts of TMA and in addition to C_8 glycidyl ether, leads to distinct changes of melting temperature (T_m) and glass transition temperature (T_g). A typical DSC scan is shown in Fig. 3. Relevant data, including blends with modified PA, are listed in Table 2. For PA samples modified with 10 or 15 wt.% of TMA both T_m and T_g are lower than in unmodified PA. This decrease in glass transition and melting temperature might result from the combined effect of some degradation of the polymer and the less perfect crystal

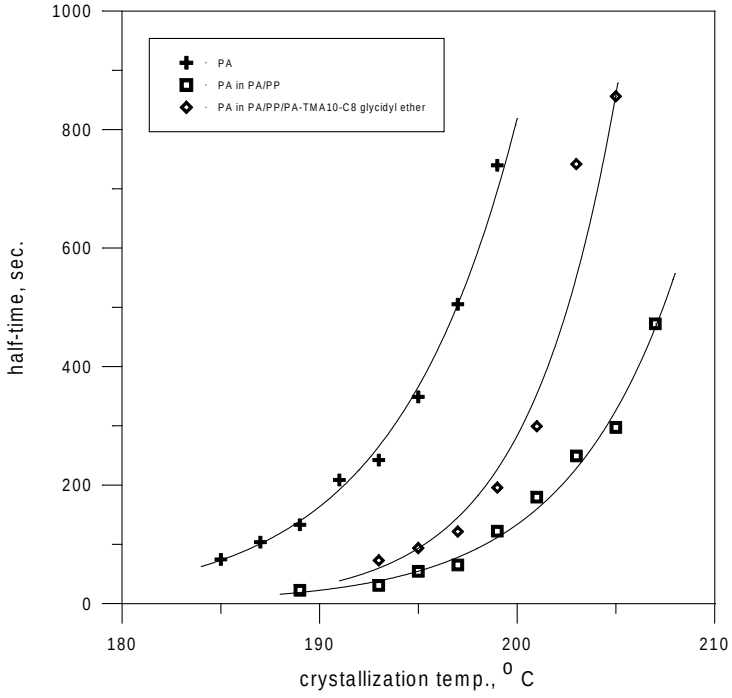

Fig. 4. Half-times of crystallization versus crystallization temperature for neat PA and in blends.

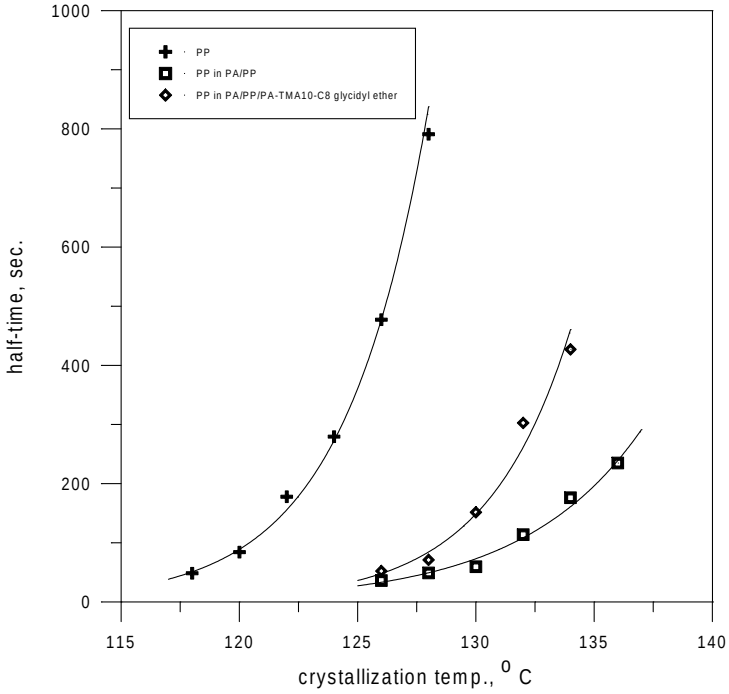

Fig. 5. Half-times of crystallization versus crystallization temperature for neat PP and in blends.

formation in the modified polymer due to bulky anhydride groups attached to the PA backbone. In contrast, a small amount of trimellitic anhydride (PA–TMA1.1) caused a slight increase in the melting temperature and more pronounced increase in glass transition temperature.

For studies of crystallization kinetics, the polymers were exposed to thermal histories described in Section 2. Half-times of crystallization, $t_{0.5}$, of PA, PP and blends of them as a function of crystallization temperature are shown in Figs. 4 and 5. The values of $t_{0.5}$ were estimated from the area of the crystallization peak at the respective crystallization temperature, T_c. An exponential increase of half-times with crystallization temperature may be recognized. Moreover, the crystallization rates, $t_{0.5}^{-1}$, at fixed crystallization

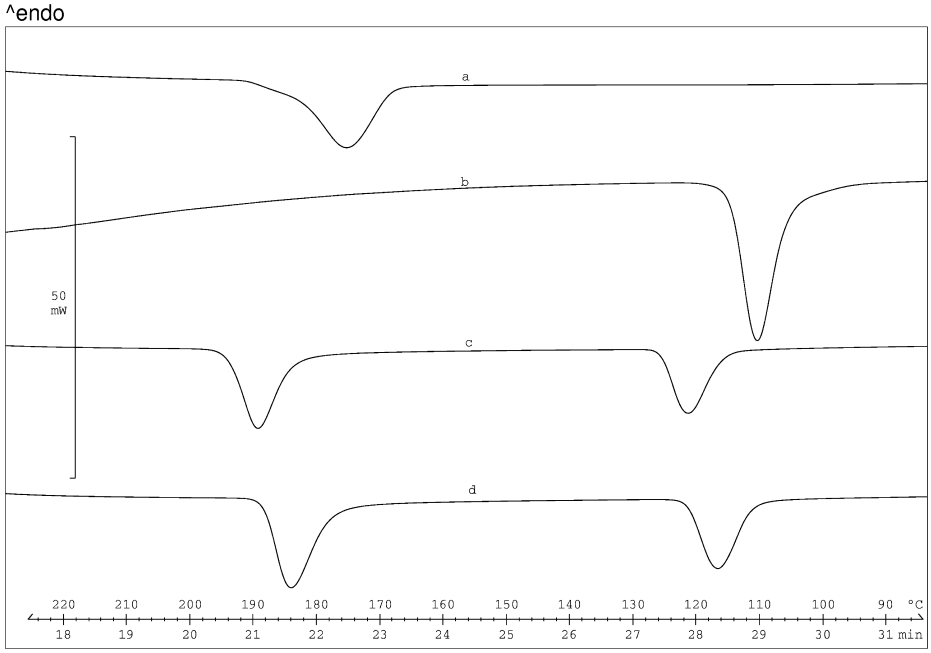

Fig. 6. DSC cooling traces for PA, PP and blends; cooling rate -10 K min^{-1}: (a) PA; (b) PP; (c) PA/PP (70/30) blend and (d) PA/PA–TMA10–C_8 glycidyl ether/PP (1/1/1) blend.

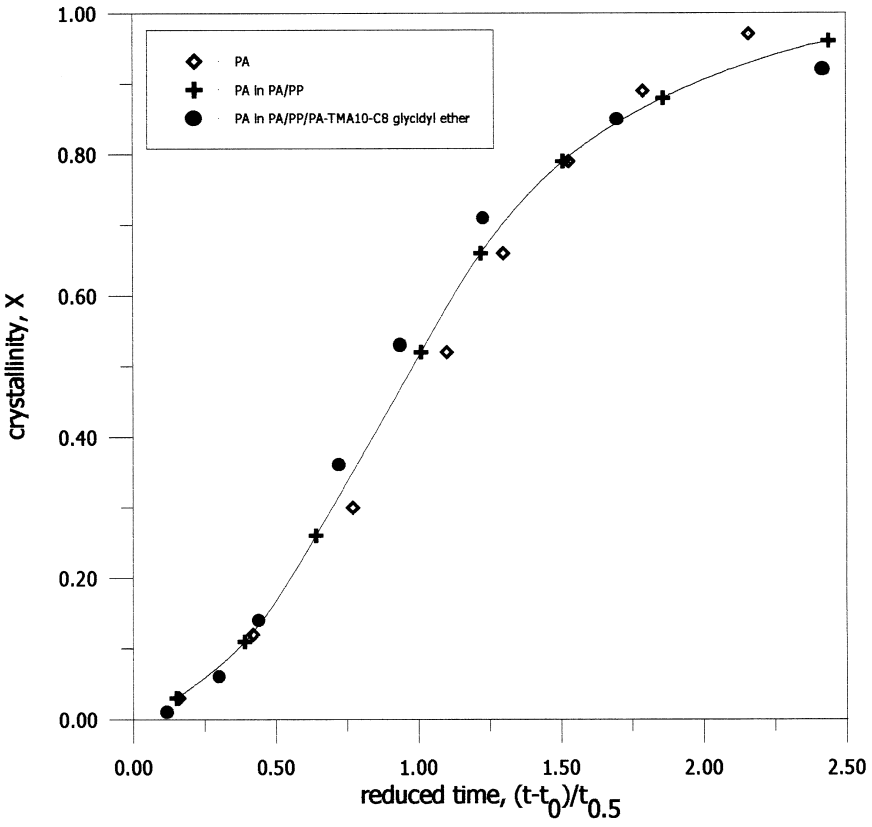

Fig. 7. Normalized crystallinity versus reduced time $(t - t_0)/t_{0.5}$ for PA at $T_c = 193$°C.

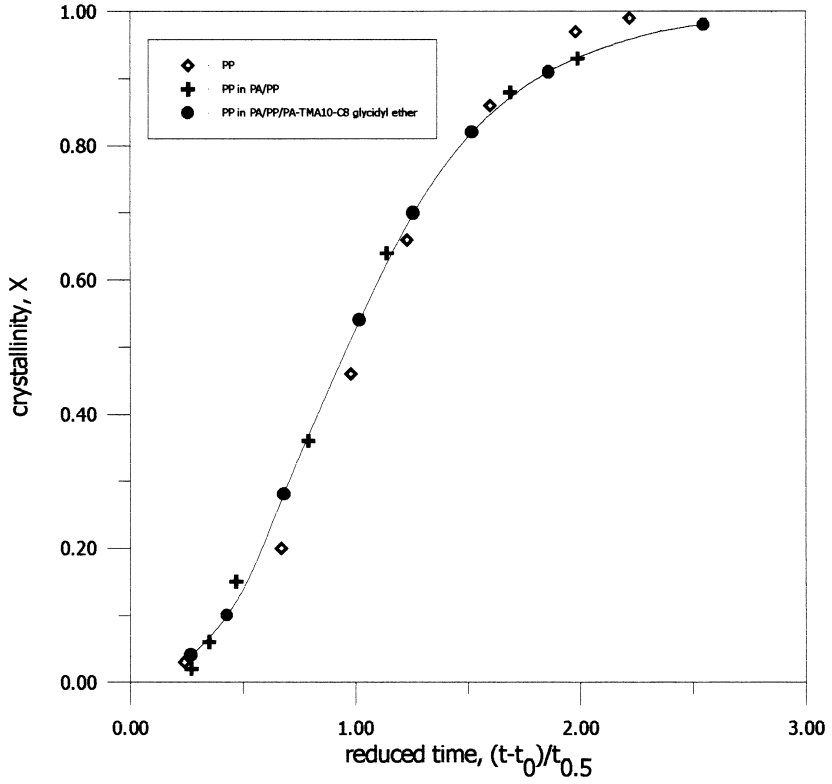

Fig. 8. Normalized crystallinity versus reduced time $(t - t_0)/t_{0.5}$ for PP at $T_c = 126$°C.

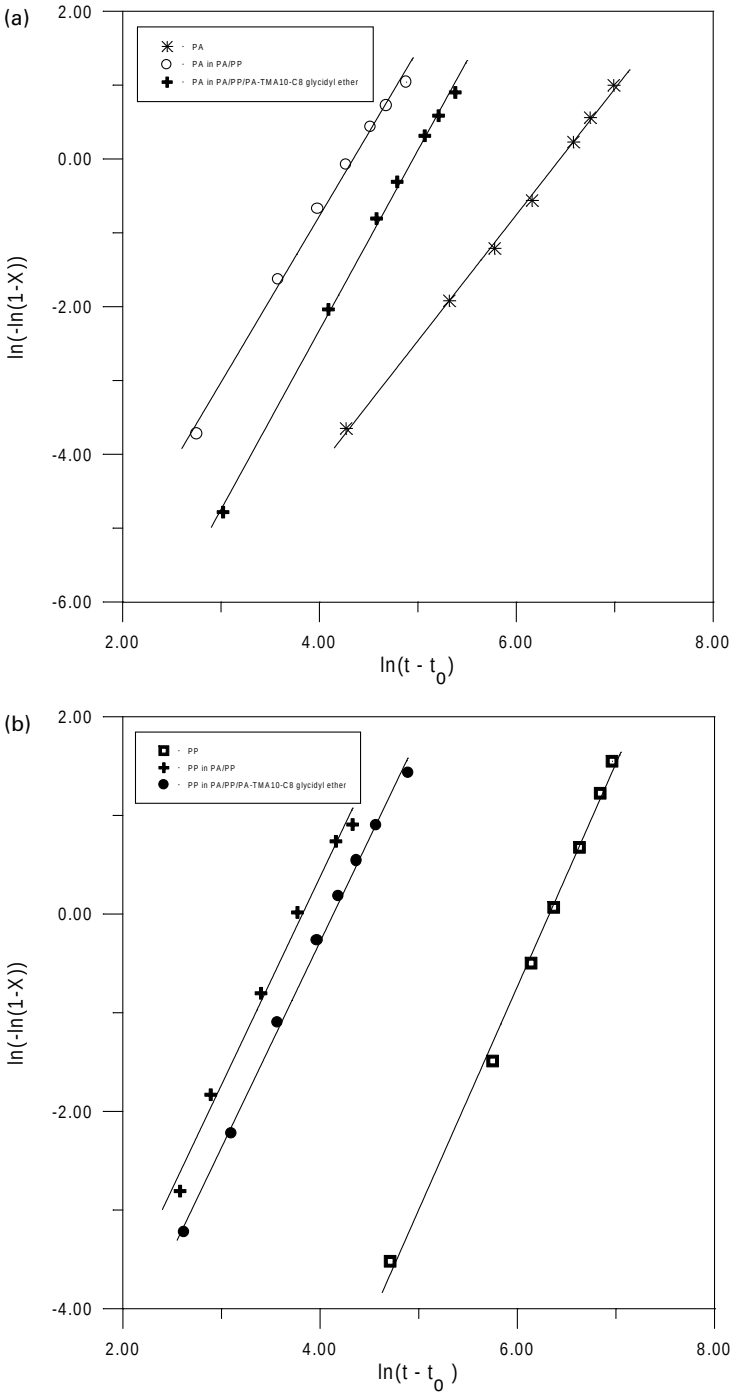

Fig. 9. (a) Avrami plots for PA at $T_c = 193$°C. (b) Avrami plots for PP at $T_c = 126$°C.

temperature are highest for both polymers in unmodified blends and slightly decrease in modified systems. Figs. 4 and 5 also demonstrate that comparable half-times of homopolymers occur in different ranges of crystallization temperature. This situation does not change in blends. Accordingly, PA crystallizes separately from PP at high temperatures. The DSC cooling traces shown in Fig. 6 explicitly explains this fact. After isothermal crystallization of PA, isothermal crystallization of PP proceeds at considerably lower temperatures. There might be some additional crystallization of PA during crystallization of PP, i.e. it is not possible to separate strictly the crystallization processes at low temperatures. However, the final crystallinities given in Table 2 reveal that the degree of crystallinity of PA in blends is slightly lower than that in neat PA. This may support the assumption that additional crystallization of PA during isothermal crystallization of PP is negligible to a good approximation.

Table 3
Averages of Avarmi exponents in the indicated range of crystallization temperatures

Sample	$\bar{n}_A$	Range of T_c (°C)
PA, neat	1.9	185–199
PP, neat	2.3	116–128
PA/PP (70/30)		
PA	2.2	189–207
PP	2.0	126–136
PA/PP/PA–TMA10–C_8 glycidyl ether (1/1/1) blend		
PA	2.2	193–205
PP	2.1	126–134

Table 4
Overall rate constants and Avrami exponents for neat polymers and blends at the indicated crystallization temperatures T_c and undercoolings ΔT

Sample and condition	K_A ($\min^{-n_A}$)	n_A
PA ($T_c = 193$°C, $\Delta T = 37$°C)		
Neat	2.7×10^{-11}	1.9
PA/PP (70/30)	4.2×10^{-7}	1.8
PA/PP/PA–TMA10–C_8 glycidyl ether (1/1/1)	4.5×10^{-9}	1.9
PP ($T_c = 126$°C, $\Delta T = 82$°C)		
Neat	4.8×10^{-15}	2.3
PA/PP (70/30)	8.8×10^{-9}	2.1
PA/PP/PA–TMA10–C_8 glycidyl ether (1/1/1)	2.3×10^{-9}	2.1

The equilibrium melting temperature of PP was determined to $T_m^\circ = 208$°C [14]. As Fig. 5 indicates, the half-time ($t_{0.5}$) of PP is so high for crystallization temperatures $T_c > 190$°C that PP is not able to crystallize in experimental times at those temperatures. This allows us to study the crystallization kinetics of PA when molten PP is present. Normalized degrees of crystallinity X determined under isothermal conditions, are plotted versus reduced time $(t - t_0)/t_{0.5}$ for $T_c = 193$°C in Fig. 7. Quantity t_0 denotes the induction period which was determined experimentally and defined as the time after which the first deviation of the DSC trace from the base line could be detected in an isothermal crystallization experiment. As can be seen, the crystallinities of neat PA and of PA in different blends coincide and form a master curve to a good approximation when X is plotted against the reduced time. This result indicates that overall features of PA crystallization do not change in blends with PP. The same result was found when developing crystallinities of neat PP and in blends with PA are depicted as a function of reduced time. An example for $T_c = 126$°C is given in Fig. 8. Again, the crystallinities in pure PP and in blends form a master curve revealing that also for PP the overall features of crystallization do not change in blends with PA. Figs. 7 and 8 show that crystallization kinetics of PA as well as of PP follow the Avrami equation [16]:

$$X(t) = 1 - \exp[-K_A(t - t_0)^{n_A}] \quad (1)$$

The normalized crystallinity $X(t)$ is defined as the ratio of peak areas $a(t)/a(\infty)$, or the ratio of degree of crystallinity at

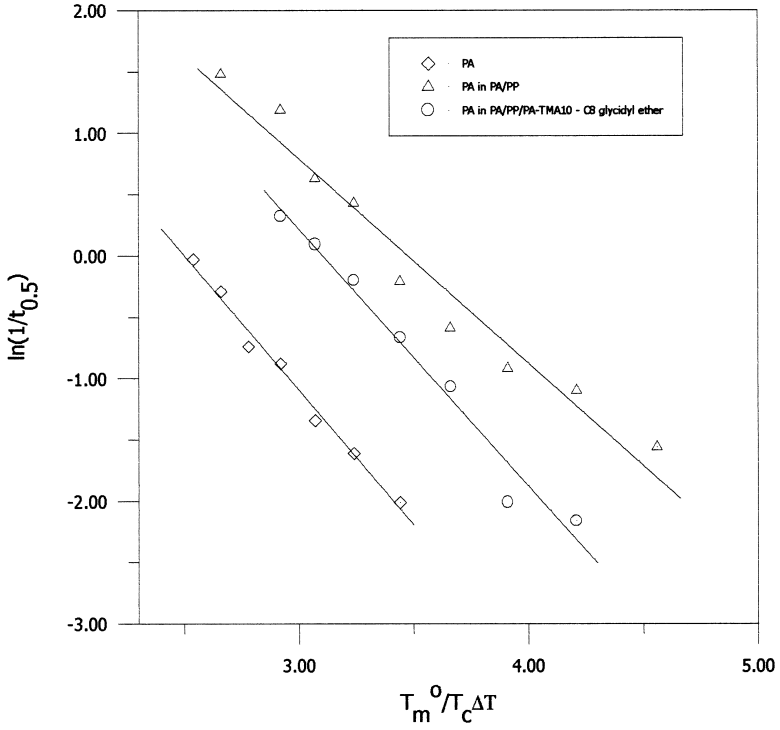

Fig. 10. Plots of rate of crystallization, $t_{0.5}^{-1}$, versus $T_m^\circ/T_c\Delta T$ for neat PA and in blends.

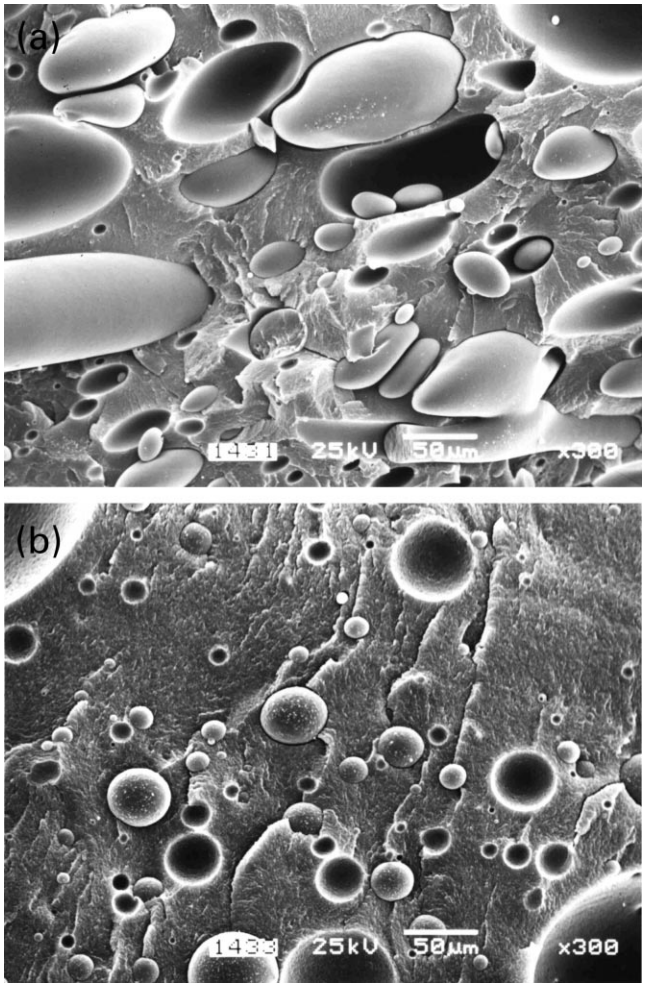

Fig. 11. SEM micrographs of PA/PP blends: (a) unmodified 70/30 blends; (b) modified blends PA/PP/PA–TMA10–C_8 glycidyl ether (1/1/1).

time t and the final degree of crystallinity. Quantities K_A and n_A represent the overall rate constant and the Avrami exponent, respectively. Selected examples for Avrami plots are given in Fig. 9. Linear relationships can be seen up to high degrees of conversion that allow to estimate quantities K_A and n_A. Avrami exponents are always close to 2 and do not change significantly neither with crystallization temperature nor with blend composition. Average values for Avrami exponents over the range of crystallization temperatures are listed in Table 3. Table 4 gives selected examples of overall rate constants and Avrami exponents. One recognizes that the overall rate constants for both polymers are highest in unmodified blends and are reduced in modified blends.

Table 5
Values of quantity K_g for PA

Sample	K_g/K	r[a]
PA	100 ± 10	0.994
PA in PA/PP (70/30)	70 ± 10	0.981
PA in PA/PP/PA–TMA10–C_8 glycidyl ether (1/1/1)	90 ± 20	0.987

[a] Correlation coefficient.

As mentioned above, only PA crystallizes separately at sufficiently high temperatures. This corresponds also to low undercoolings, $\Delta T = T^\circ_m - T_c$, where the equilibrium melting temperature of PA is assumed to be $T^\circ_m = 230$°C [13]. Under these conditions, one can study the influence of the molten PP phase on the crystallization of PA. We analyzed the rate of crystallization, expressed by reciprocal half-times, $t_{0.5}^{-1}$, in terms of Hoffman's theory [17]. Accordingly, the rate of crystallization, at which crystallinity develops from the melt, follows an Arrhenius-like relationship. The corresponding activation energy comprises two contributions, one for transport of the chain molecules towards the growing nuclei and the other one for nucleation. Since it is difficult to separate precisely these two contributions, we cast the equation here in the simplified version:

$$t_{0.5}^{-1} \propto \exp\left(-K_g \frac{T^\circ_m}{T_c \Delta T}\right) \quad (2)$$

where K_g represents a temperature and RK_g corresponds to an activation energy at a certain crystallization temperature. The rate of crystallization increases at T_c = constant with descending K_g. After Eq. (2), plots of $\ln(t_{0.5}^{-1})$ versus $T^\circ_m/T_c\Delta T$ should give straight lines with slope K_g. The results for PA are shown in Fig. 10. The accuracy of the regression coefficients was statistically analyzed in terms of a t-test at 95% confidence interval. Relevant quantities, calculated from the slopes, are listed in Table 5. We note that temperature coefficient K_g of PA is higher in neat PA than in the unmodified blend, whereas K_g of the modified blend is somewhere in between these two values. However, no significant differences could be observed for K_g of the modified blend neither to neat PA nor to the unmodified blend.

3.3. Morphology and interfacial properties

Morphology analysis revealed clear differences between PA/PP (70/30) and PA/PP/PA–TMA10–C_8 glycidyl ether (1/1/1) blends. The noncompatibilized, binary reference blend (Fig. 11a) exhibits a very inhomogeneous fracture surface, indicating poor adhesion between PA and PP phases. The dispersed phase particles are large and irregularly shaped. Fig. 11b illustrates how the dispersed particle size changes when a part of PA is modified with TMA and C_8 glycidyl ether. There is evidence of spherical domains much smaller in size. In a first approximation, one may say that the size of the dispersed phase in a molten polymer blend subjected to shear is determined by the viscosity ratio of the components and the ratio between interfacial tension and the product of local shear stress and particle radius. Thus, if viscosities of the components and processing parameters are fixed, interfacial tension is the prominent factor that governs blend morphology.

Table 6
Surface tension of polymers

Sample	Temperature (°C)	Surface tension (mN/m)	Interfacial tension (mN/m)
PA	25	47.6	
PA–TMA10–C_8 glycidyl ether	25	44.5	
PP	235	17.6	
PA	235	41.3	
PA–TMA10–C_8 glycidyl ether	235	38.8	
PP/PA	235		9.0
PP/PA–TMA10–C_8 glycidyl ether	235		1.8

Surface tensions of PA and PA–TMA10–C_8 glycidyl ether at room temperature were determined from advancing contact angles (θ) on 1-mm thick polymer films applying Young's equation in geometric mean approximation. Young's equation reads when one neglects the spreading pressure as:

$$\gamma_s - \gamma_{sl} = \gamma_l \cos\theta \quad (3)$$

where γ_s and γ_l are the surface tensions of solid and liquid, respectively, and γ_{sl} is the solid–liquid interfacial tension. The approximation $\gamma_{sl} = (\sqrt{\gamma_s} - \sqrt{\gamma_l})^2$ leads eventually to

$$(1 + \cos\theta_i)\gamma_i = 2[(\gamma_i^d \gamma_s^d)^{1/2} + (\gamma_i^p \gamma_s^p)^{1/2}] \quad (4)$$

Superscripts d and p correspond to dispersive and polar components of the surface energy, respectively. As can be seen from Table 6, introducing C_8-alkyl groups into the polyamide chain reduces the surface tension at room temperature from 47.6 to 44.5 mN/m for unmodified and modified PA, respectively. This reduction in surface tension was also confirmed at higher temperatures. Molten PA–TMA10–C_8 glycidyl ether wetted the PP surface better than unmodified PA. The corresponding contact angle decreases from 78° for the unmodified to 66° for the modified sample. Eq. (3) allows to estimate interfacial tension γ_{sl} between the polymers. Contact angle measurements were carried out at 235°C under conditions described in Section 2. Accordingly, quantity γ_l is here the surface tension of molten polyamide. It was estimated from $\gamma_{PA} = 37.8$ mN/m at 280°C and $d\gamma/dT = -0.101$ mN/(m K) [18]. The surface tension of molten polypropylene is taken as γ_s. It was calculated from $\gamma_{PP} = 20.8$ mN/m at 180°C and $d\gamma/dT = -0.058$ mN/(m K) [19]. Data for PA–TMA10–C_8 glycidyl ether at 235°C, not available in the literature, was taken as 0.94 of the surface tension of molten PA. This corresponds to the ratio $\gamma_{PA-MA10-C8\ glycidyl\ ether}/\gamma_{PA}$ measured at room temperature. The estimation of interfacial tension between PA and PP, $\gamma_{PA/PP}$, via Eq. (3) demonstrates a significant decrease of interfacial tension in modified blends (cf. Table 6). This result is in qualitative agreement with Fig. 11 displaying a finer dispersion of the droplet phase in modified blends as compared to unmodified systems.

Fig. 12 shows the yield stress of binary blends of polyamide and polypropylene as well as of PA/PP blends containing additionally 10 wt.% of polyamide was replaced by PA–TMA10–C_8 glycidyl ether. As expected the yield stress of blends is considerably lower over the whole

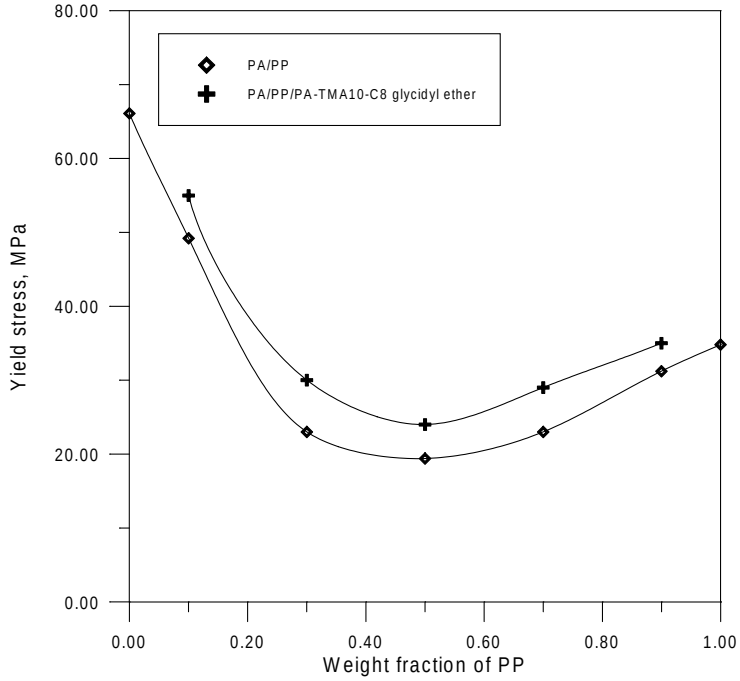

Fig. 12. Yield stress as a function of weight fraction of PP for unmodified and modified blends.

composition range as compared to that of the pure components. The addition of the modified polyamide causes smaller depression of yield stress. It could be due to location of modified PA with C_8-alkyl groups at the interface, acting as an interfacial agent. Thus, higher homogeneity is achieved with respect to unmodified binary blends. This morphology contributes to a decrease of high stress concentration around the dispersed particles (making the system more efficient) so reducing the tendency for premature rupture.

4. Conclusion

In conclusion, there is evidence that the modified PA acts as compatibilizing agent in PA/PP blends. Compared to unmodified blends, the rates of crystallization of the polymers are reduced in modified blends. Moreover, interfacial tension is observed to be lower between molten PP and modified PA than between PP and PA. This is consistent with occurrence of finer particle distributions in modified systems compared to unmodified blends. These results point to compatiblizing effects of the modified PA.

Acknowledgements

The authors are grateful for financial support by the Komitet Badan Naukowych, Poland (Grant no. 3 T09B 094 13).

References

[1] Park JS, Kim BK, Jeong HM. Eur Polym J 1990;26:131.
[2] Mülhaupt R, Rösch J. Kunststoffe 1994;84:1153.
[3] Gonzalez-Montiel A, Keskkula H, Paul DR. Polymer 1995;36:4587.
[4] Li H, Chiba T, Higashida N, Yang Y, Inoue T. Polymer 1997;38:3921.
[5] Holsti-Miettinen RM, Seppälä JV, Ikkala OT, Reima IT. Polym Engng Sci 1994;34:395.
[6] Ide F, Hasegawa A. J Appl Polym Sci 1974;18:963.
[7] Al.-Malaika S, editor. Reactive modifiers for polymers London: Blackie Academic, 1997.
[8] Serpe G, Jarrin J, Dawans F. Polym Engng Sci 1990;30:553.
[9] Eichhorn KJ, Lehmann D, Voigt D. J Appl Polym Sci 1996;62:2053.
[10] Marechal P, Coppens G, Legras R, Dekononck JM. J Polym Sci A, Polym Chem 1995;33:757.
[11] Oshinski AJ, Keskkula H, Paul DR. Polymer 1992;33:268.
[12] Okada O, Keskkula H, Paul DR. Polymer 1999;40:2699.
[13] Campoy I, Arribas JM, Zaporta MAM, Marco C, Gomez MA, Fatou JG. Eur Polym J 1995;31:475.
[14] Fatou JG. Eur Polym J 1971;31:475.
[15] Brandrup J, Immergut EH. Polymer handbook. 3rd ed.. New York: Wiley, 1989.
[16] Avrami M. J Chem Phys 1939;7:1003.
[17] Hoffman JD. Polymer 1982;24:3.
[18] Kammer HW. Z Phys Chem. Leipzig 1977;258:1149.
[19] Wu S. Polymer interface and adhesion. New York: Marcel Dekker, 1982.